SMC-TR-95-39

AEROSPACE REPORT NO.
TR-95(5925)-2

Characterization of Porosity Distributions of Slurry-Coated and Dry-Powder Plaques Using Conductive Image Technique

15 January 1995

Prepared by

A. H. PHAN, A. H. ZIMMERMAN, and M. V. QUINZIO
Electronics Technology Center
Technology Operations

Prepared for

SPACE AND MISSILE SYSTEMS CENTER
AIR FORCE MATERIEL COMMAND
2430 E. El Segundo Boulevard
Los Angeles Air Force Base, CA 90245

Engineering and Technology Group

THE AEROSPACE CORPORATION
El Segundo, California

This report was submitted by The Aerospace Corporation, El Segundo, CA 90245-4691, under Contract No. F04701-88-C-0089 with the Space and Missile Systems Center, Los Angeles Air Force Base, CA 90245. It was reviewed and approved for The Aerospace Corporation by T. A. Galantowicz, Principal Director, Electronics Technology Center. Maj. J. W. Cole was the project officer for the Mission-Oriented Investigation and Experimentation (MOIE) program.

This report has been reviewed by the Public Affairs Office (PAS) and is releasable to the National Technical Information Service (NTIS). At NTIS, it will be available to the general public, including foreign nationals.

This technical report has been reviewed and is approved for publication. Publication of this report does not constitute Air Force approval of the report's findings or conclusions. It is published only for the exchange and stimulation of ideas.

MAJ. J. W. COLE
SMC/SDE

REPORT DOCUMENTATION PAGE

Form Approved
OMB No. 0704-0188

1. AGENCY USE ONLY (*Leave blank*)	2. REPORT DATE	3. REPORT TYPE AND DATES COVERED
	15 January 1995	

4. TITLE AND SUBTITLE
Characterization of Porosity Distributions of Slurry-Coated and Dry-Powder Plaques Using Conductive Image Technique

5. FUNDING NUMBERS
F04701-93-C-0094

6. AUTHOR(S)
A. H. Phan, A. H. Zimmerman, and M. V. Quinziio

7. PERFORMING ORGANIZATION NAME(S) AND ADDRESS(ES)
The Aerospace Corporation
Technology Operations
El Segundo, CA 90245-4691

8. PERFORMING ORGANIZATION REPORT NUMBER
TR-95(5925)-2

9. SPONSORING/MONITORING AGENCY NAME(S) AND ADDRESS(ES)
Space and Missile Systems Center
Air Force Materiel Command
2430 E. El Segundo Boulevard
Los Angeles Air Force Base, CA 90245

10. SPONSORING/MONITORING AGENCY REPORT NUMBER
SMC-TR-95-39

11. SUPPLEMENTARY NOTES

12a. DISTRIBUTION/AVAILABILITY STATEMENT
Approved for public release; distribution unlimited

12b. DISTRIBUTION CODE

13. ABSTRACT (*Maximum 200 words*)

The porosity distributions of sinter plaques manufactured by dry powder and wet slurry processes were measured using an improved conductive imaging microprobe This study has indicated that the pore size distributions of dry-powder plaques are more uniform than those of the slurry-coated plaques. For the slurry process, porosity distribution depends on many variables (such as slurry viscosity and density, sinter temperature,and processing speed), and the pore size distribution can have significant spatial variability if the sintering conditions deviate significantly from the optimum. The results also suggest that for wet-slurry sinter, better process optimization could be obtained by properly controlling the above-mentioned parameters to obtain more uniform and reproducible slurry coats.

14. SUBJECT TERMS	15. NUMBER OF PAGES
Porosity distributions, Plaques, Sinter temperature, Slurry	15
	16. PRICE CODE

17. SECURITY CLASSIFICATION OF REPORT	18. SECURITY CLASSIFICATION OF THIS PAGE	19. SECURITY CLASSIFICATION OF ABSTRACT	20. LIMITATION OF ABSTRACT
UNCLASSIFIED	UNCLASSIFIED	UNCLASSIFIED	

NSN 7540-01-280-5500

Standard Form 298 (Rev. 2-89)
Prescribed by ANSI Std. Z39-18
298-102

Contents

Figures

Table

I. Introduction

Porosity distributions in nickel-sintered plaques play an important role in determining electrochemical utilization and long-term performance of nickel electrodes in nickel-hydrogen (Ni-H_2) and nickel-cadmium (Ni-Cd) cells. The pore size distributions of these plaques affect the loading level and loading uniformity of active material within the void volume. As a consequence, it is important to be able to measure the pore size and porosity distributions in different types of sintered plaques. Pore size variation effects on plate performance should be understood. If large variations are detrimental, those plaques should be excluded from the impregnation process. In this study, the characteristics of plaques from wet slurry and dry powder processes were obtained using an improved conductive imaging microprobe that has better resolution than that previously obtained (new resolution = 0.1 μm or less vs. old resolution of 0.2 μm).

II. Experimental

The conductivity imaging technique is used to measure the size of a large number of pores across the thickness of the sintered plaque. The experimental setup consists of a piezoelectric stage (model P-202X STM Sample Positioner) mounted on a servo translational stage capable of moving in two directions (X and Y, Figure 1). The STM stage allows a sample secured to the platform to be moved about 3 mm in any direction from its center position. Incremental movements of 0.1 μm or less are possible with this stage. A one-inch-long nickel plaque, potted in epoxy and cross-sectioned, is mounted on the piezoelectric stage. A platinum probe with a very fine tip (the probe tip radius is typically about 0.1 μm) is attached to another translational stage capable of moving in the Z direction, and it is positioned perpendicular to the sample. A digital-to-analog (D/A) board (model NI-DAQ AT-AO 6/10 which contains ten analog input/output channels; an onboard voltage of +10 V is available for analog output) is used to control the STM sample positioner (for fine movement) and X-Y servo motor (for coarse movement). A general-purpose interface board (GPIB) is used for data acquisition of conductivity measurements (Figure 2). The new experimental setup offers improvements over the previously used method[1,2] by having a piezoelectric translational stage capable of moving in smaller step sizes to obtain better resolution.

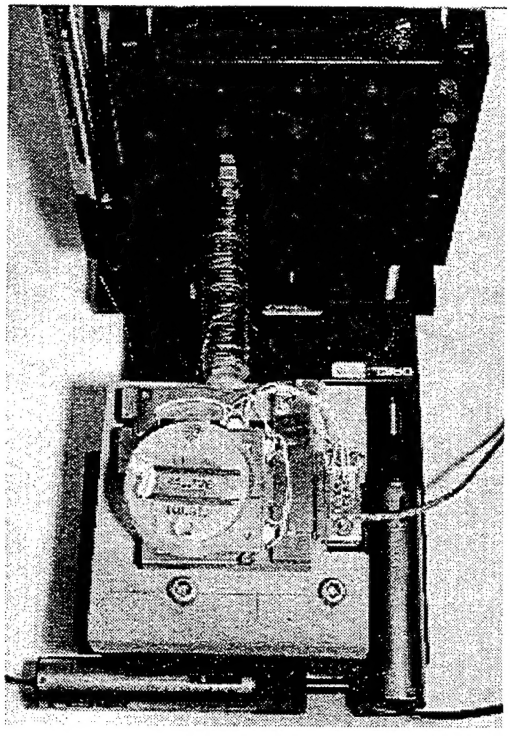

Figure 1. Precision scanning stage.

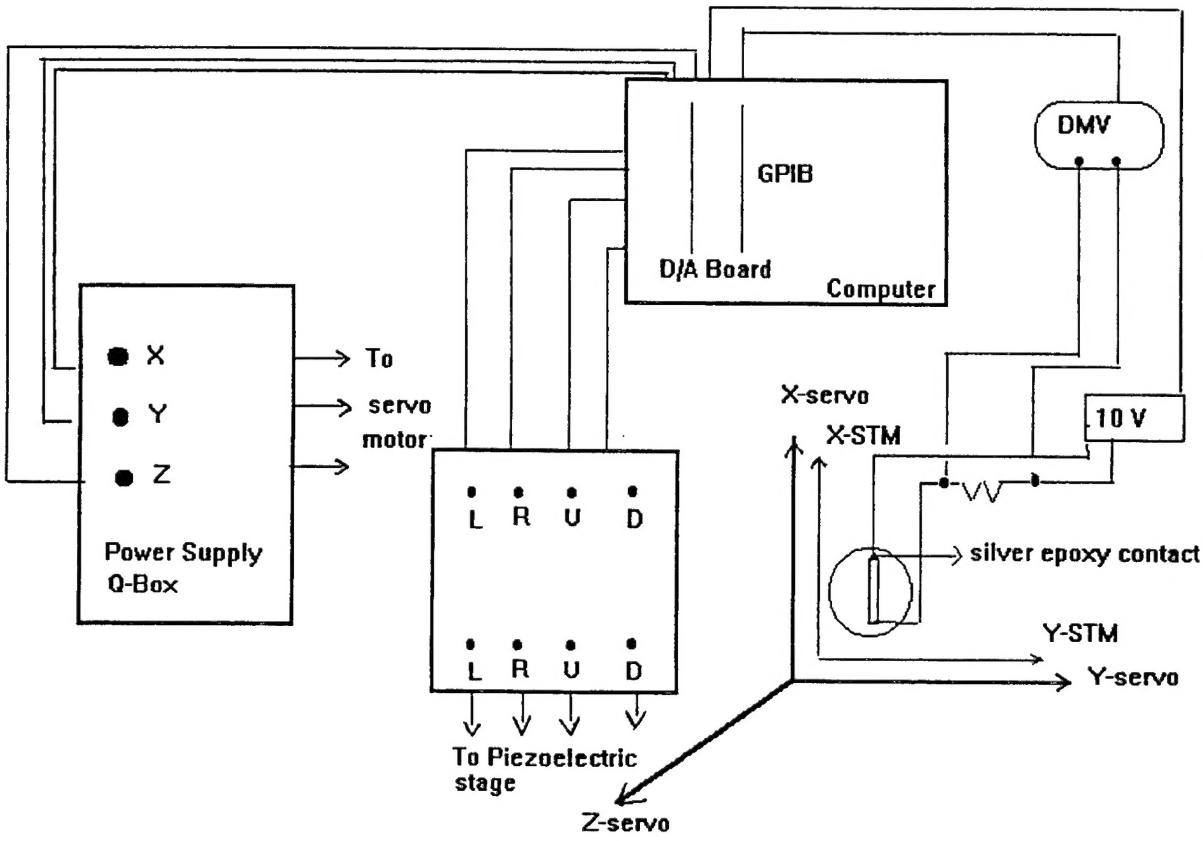

Figure 2. Conductive imaging configuration.

The dimensions, weight, and bulk porosity of dry-sintered plaques (1.2" × 0.5") were measured for use as calibration data for subsequent statistical analysis (Table 1).

Table 1. The Bulk Porosity Measurements for Dry-sintered Plaques

Sample #	Thickness (cm)	Width (cm)	Length (cm)	Weight(cm)	Solid Vol (cm^3)	Wt. Sinter (g)	Wt. Screen (g)	Plaque Porosity (%)
25-249	0.0705	1.196	3.03	0.58	0.255	0.450	0.132	74.4
25-259	0.076	1.19	3.06	0.56	0.277	0.430	0.132	77.2
25-327	0.0777	1.20	3.1	0.58	0.289	0.452	0.132	77.3
437-H2-I	0.0754	1.21	3.06	0.62	0.279	0.482	0.139	75.0
438-H2-E	0.0732	1.20	3.06	0.58	0.268	0.455	0.131	75.5
439-H2-H	0.0749	1.20	3.10	0.61	0.278	0.480	0.136	75.2
441-H2-E	0.0762	1.22	3.10	0.63	0.288	0.492	0.141	75.3
440-H2-	0.0727	1.15	3.09	0.58	0.258	0.452	0.131	74.7

During the experiment, the platinum probe is lowered to touch the sample. If the probe encounters a sinter particle, conductivity between the sample and the Pt probe will be observed. If the probe scans through a void region, no conductivity is recorded. Typically, 40–50 scans, each consisting of 6,000 to 8,000 conductivity measurements, were obtained across the width of each nickel sinter sample. These data were evaluated to determine the size of individual pores. Pore sizes were calculated in five different regions of the sinter cross-section thickness to form a pore size distribution. Statistical analysis of the data provides porosity and pore-size distributions in sintered plaques. More details on the analysis method are given in Refs. 1 and 2.

III. Results and Discussion

Eight dry powder plaques were obtained, and their porosity characteristics were measured. For dry-powder sinter, the mean pore diameter does not vary appreciably across the thickness of the plaque (from 15 to 30 μm), except for samples # 439-H2H and 438-H2E, which have a more pronounced variation (from 15 to 45 μm; see Figures 3 and 4). Figure 5 shows the comparison between the mean pore diameter distributions for dry-powder sinter and slurry-coated plaques.

Sinters obtained from the slurry process have larger pores in the interior of the plaque (≥60 μm, Ref. 2) and smaller pores near the surface as compared with those of the dry powder process (Figure 5 and Ref. 2). The presence of large pores in the center of the plaques is not desirable because large internal voids can diminish the electrode energy density. These pores do not completely fill with active material, or if filled, do not give high electrochemical utilization. Figure 5 shows that for the slurry process, the number of pores larger than 10–20 μm in the

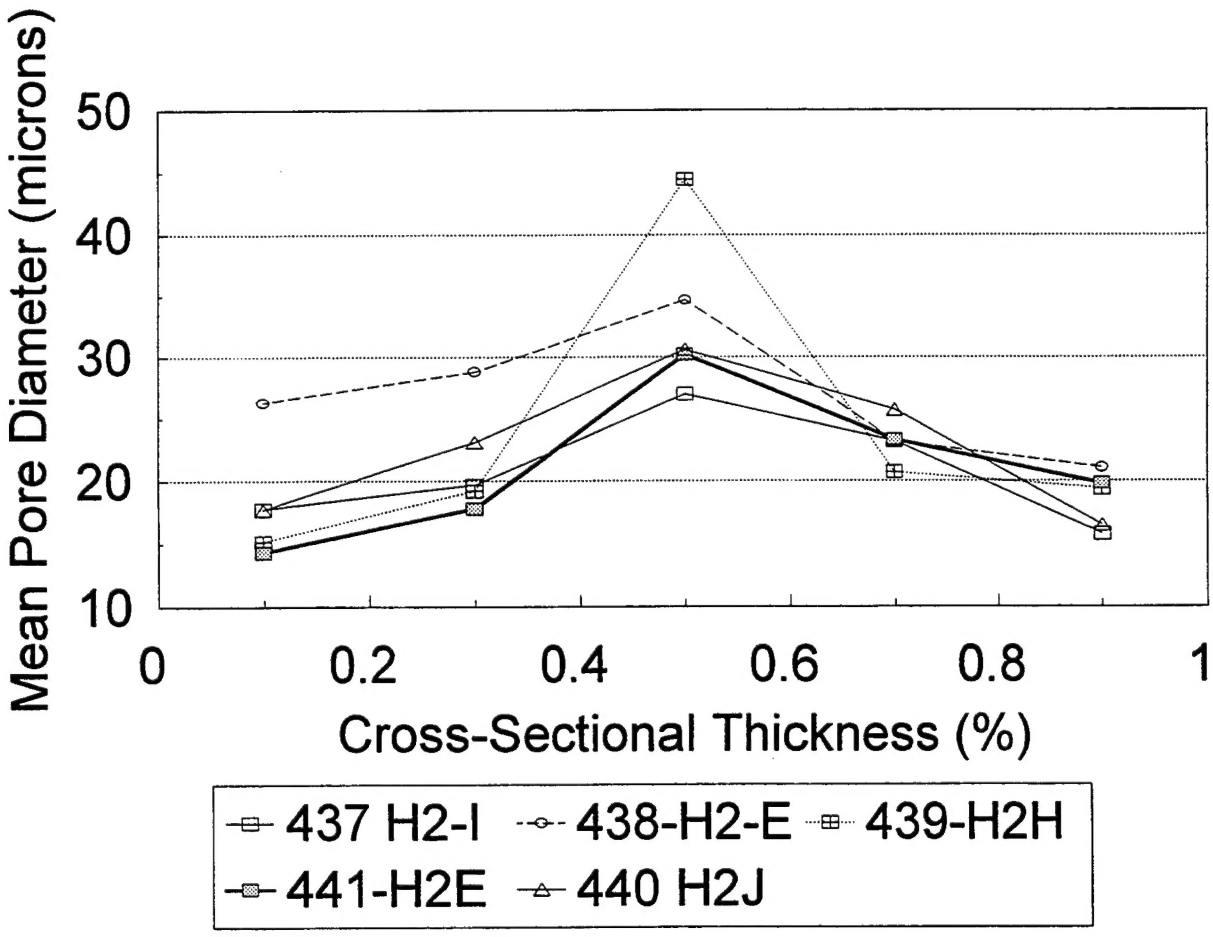

Figure 3. Mean pore diameter distribution (437-H2-I, 438-H2-E, 439-H2-H, 441-h2-E, 440-H2-J).

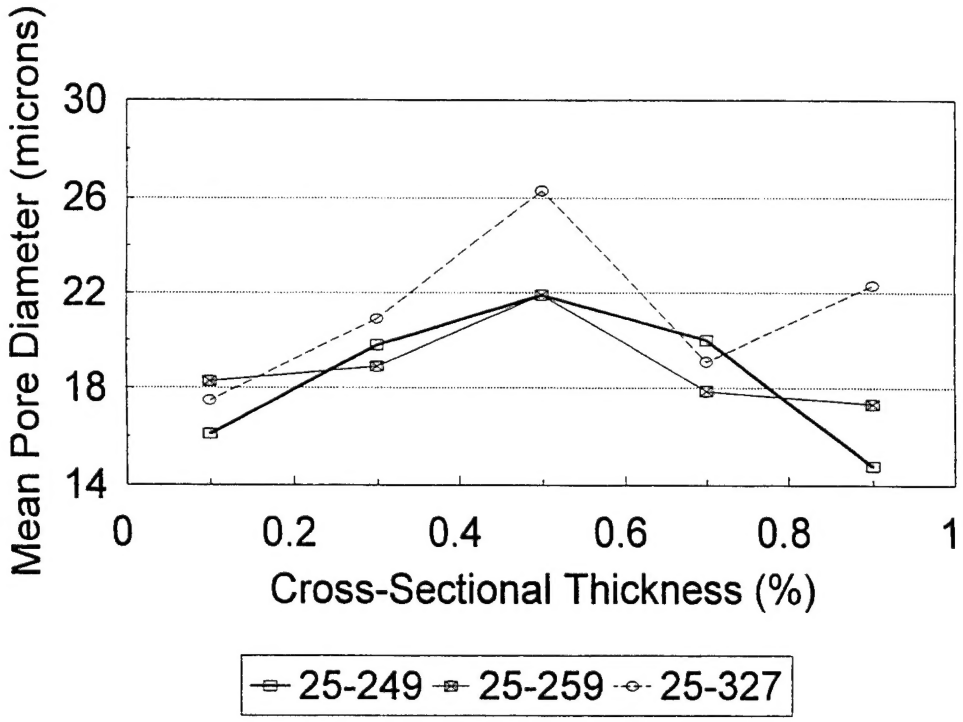

Figure 4. Mean pore diameter distribution (25-249, 25-259, 25-327).

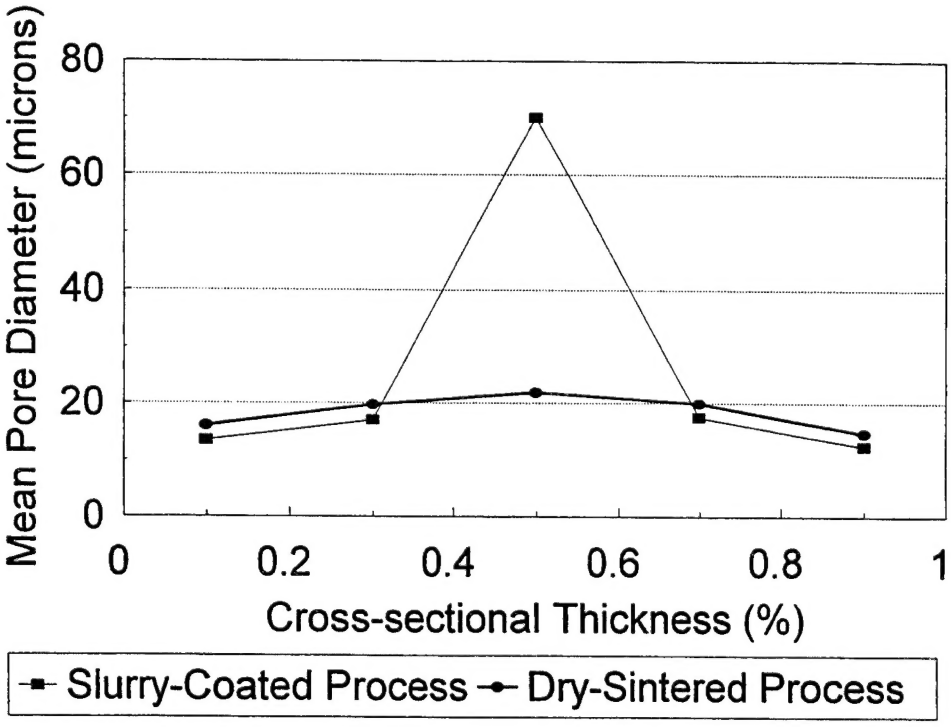

Figure 5. Mean pore diameter distribution (dry-sintered vs. slurry-coated).

central regions of the plaques is very significant, and utilization has been shown[3] to be optimum when average pore size is below approximately 20 μm, utilization decreasing sharply as the pore size increases. In practice, the pore size distribution of sintered plaque is preferred to be between 10 and 20 μm for optimum performance of the finished electrode.[3] Therefore, adjustment of the slurry process to minimize the incidence of larger pores in the inner region may be desirable.

Figures 6 and 7 indicate the relative porosity distributions for dry-powder plaques. The relative porosity distribution was calculated by correlating the average cumulative areas of pores with the known bulk porosity.[1,2] As shown in these figures, the relative porosity varies as much as 10–20% for dry-powder plaques. However, this variation is not as pronounced as that of the wet slurry plaque (Figure 8 and Ref. 2). The porosity distributions of dry-powder plaques are skewed (Figures 6 and 7) with a higher porosity on one side of the plaque. The slurry process sinter tends to have a more significant variation in porosity distribution across the thickness of the plaque. The very low porosity in the center of the slurry-coated plaque (Figure 8) results from the presence of the perforated nickel metal substrate in this region (for the dry sinter process, the substrate is a fine-mesh screen).

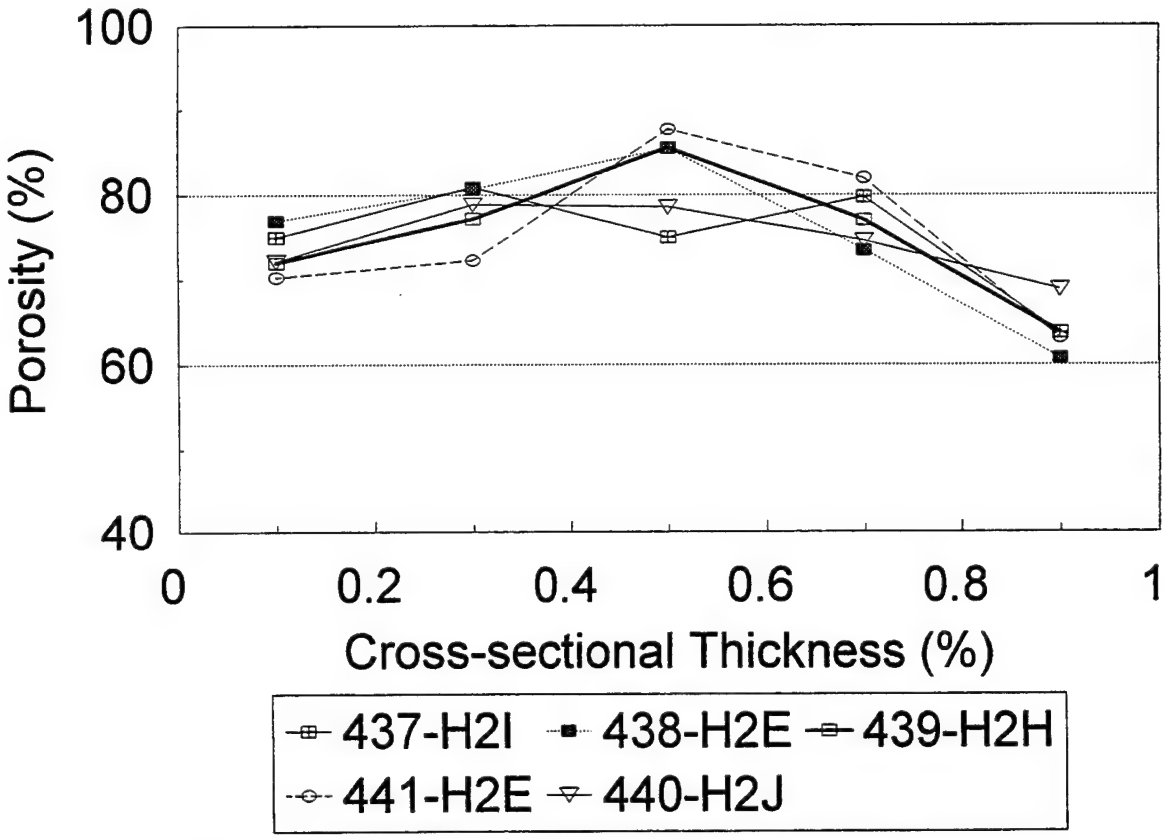

Figure 6. Porosity distribution for dry-sintered plaques (437-H2-I, 438-H2-E, 439-H2-H, 441-H2-E, 440-H2-J).

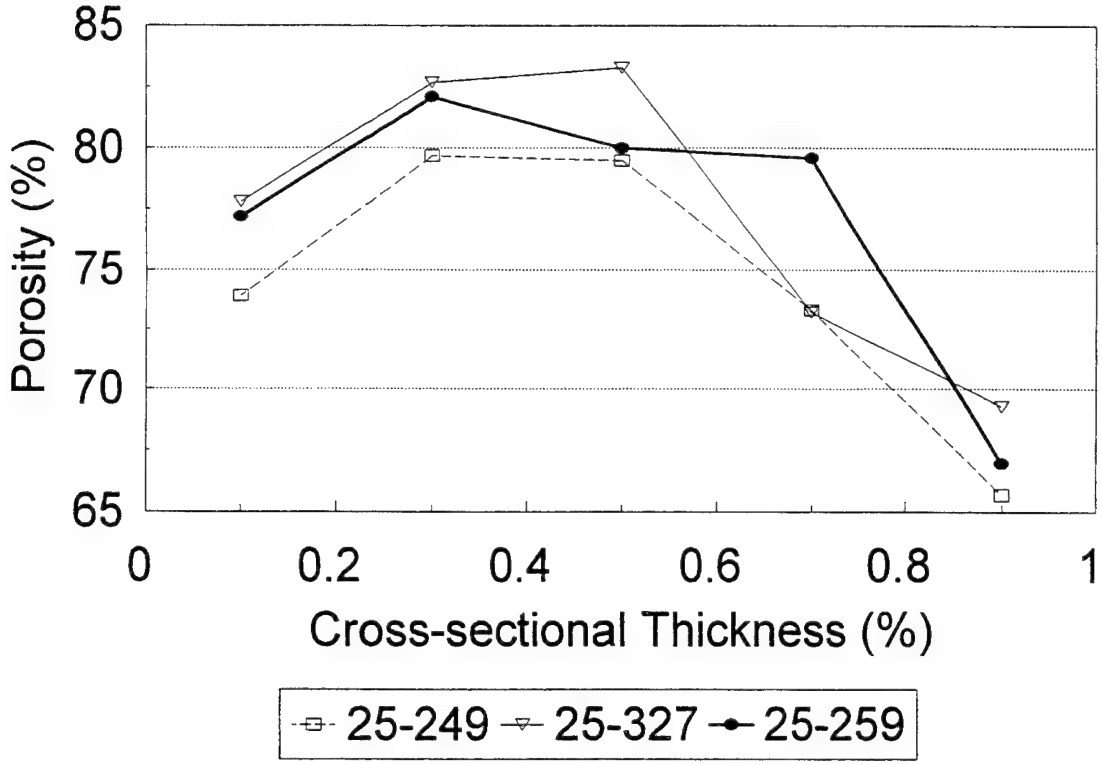

Figure 7. Porosity distribution for dry-sintered plaques (25-249, 25-327, 25-259).

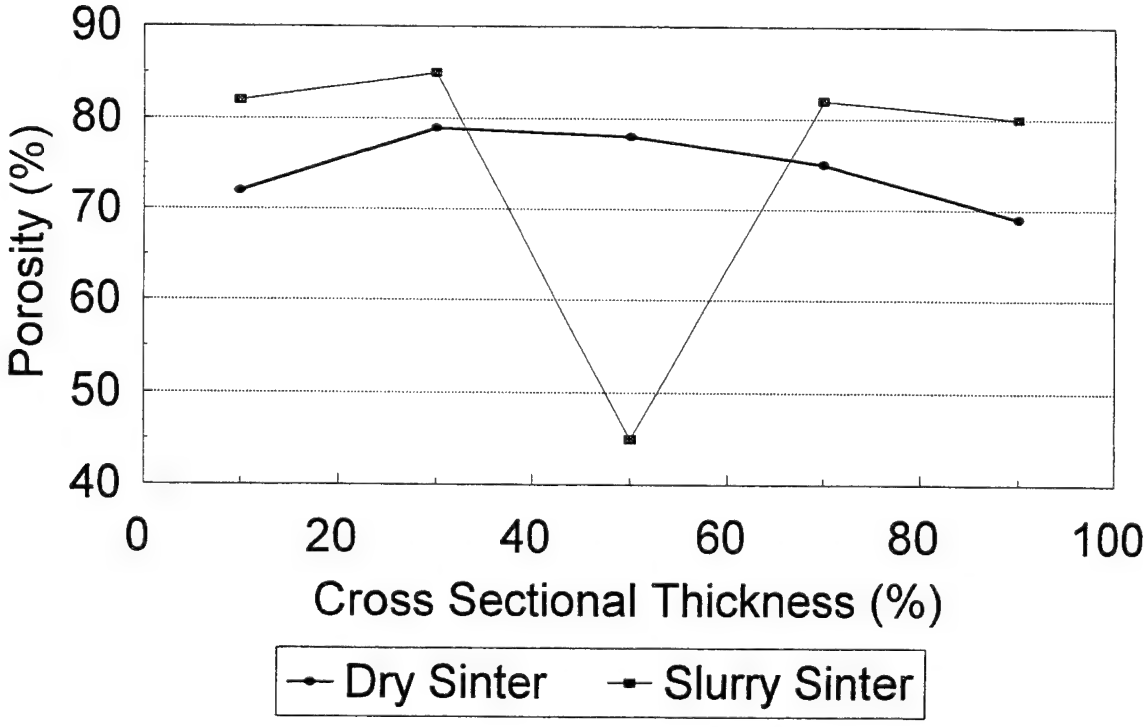

Figure 8. Typical porosity distributions for nickel plaques.

Figures 9 and 10 show plots of the distribution of the non-uniformity parameters with cross-sectional thickness. The non-uniformity is a measure of the uniformity of a certain pore size (mean diameter in this case) within any specific region of the sinter. If the non-uniformity parameter approaches a large number, it suggests that the void area is in a single pore. If the parameter is unity, it is an indication that the pores are uniform within the sinter region. As shown in Figures 9 and 10, the pore sizes of these dry-sinter plaques are relatively uniform across the thickness (non-uniformity parameter ≤6), except for samples # 441-H2E, 439-H2E, and 25-327. For the dry-sinter plaques used in this study, generally, the fraction of pores having diameters close to the mean diameter (15–20 μm) is significant, which is a desirable pore size distribution.

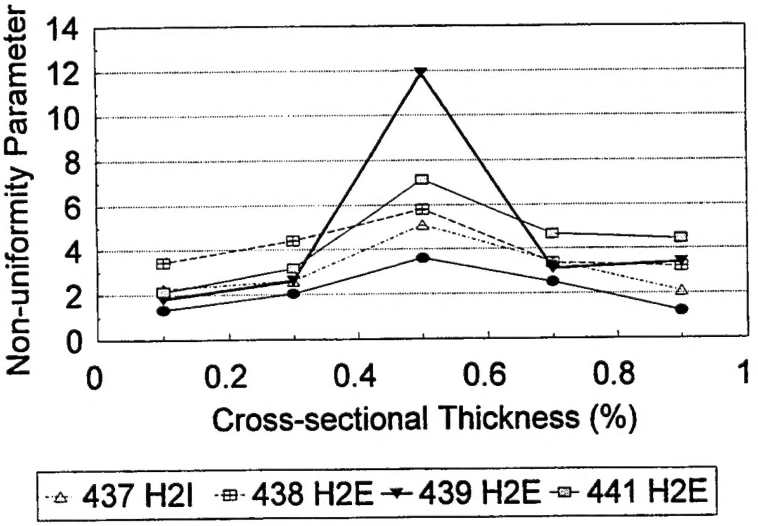

Figure 9. Non-uniformity parameter distribution for dry-sintered plaques (437-H2-I, 438-H2-E, 439-H2-E, 441-H2-E).

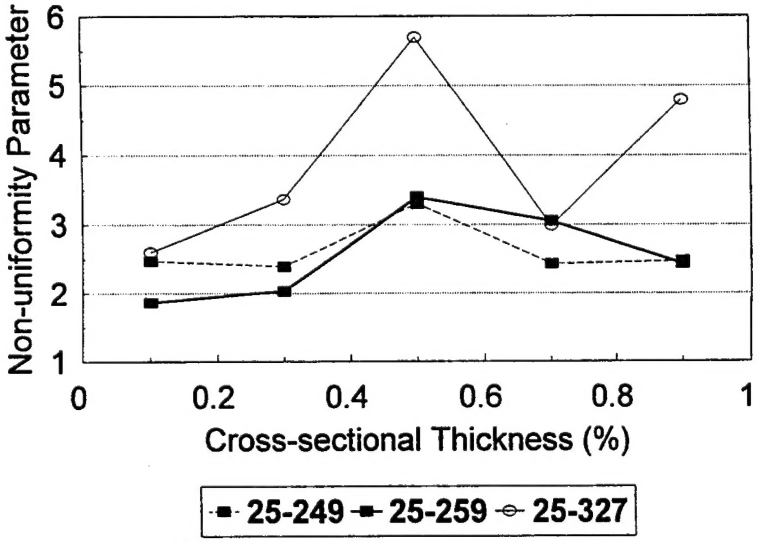

Figure 10. Non-uniformity parameter distribution for dry-sintered plaques (25-249, 25-259, 25-327).

IV. Summary and Recommendations

The improved conductive imaging technique, developed within the Energy Technology Department, provides an effective tool for the determination of porosity and pore-size distributions of unimpregnated plaque materials. This technique helps characterize the porosity variation for different production conditions or for diverse manufacturing methods. It is possible to characterize the differences in porosity distributions for plaques made from slurry and dry powder processes by using this technique. The dry and slurry sintering processes have been used for many years, and both are in current use for the manufacturing of aerospace nickel electrodes. Our study has indicated that the pore size distributions of dry-powder plaques are more uniform than those of the slurry-coated plaques. The results suggest that for wet-slurry sinter, better process optimization could be obtained by properly and carefully controlling the slurry viscosity and density and sinter conditions to obtain more uniform and reproducible slurry coats. This technique, the methods of interpretation, and results are currently available to sintered-plaque manufacturers to allow and encourage them to utilize this new capability for quality control in their sintering processes.

References

1. A. H. Zimmerman, "Pore Size Distribution Measurements for Sintered Nickel Substrates," ATM-91(6925-11)-4.

2. N. H. Phan, A. H. Zimmerman, and M.V. Quinzio, "Porosity Distribution Measurements for Welsh and Canadian Nickel Sintered Substrates," ATM 93.(3925-09)-7.

3. W. R. Scott and D. W. Rusta, "Sealed-cell Nickel-Cadmium Battery Application Manual," NASA Reference Publication 1052.

TECHNOLOGY OPERATIONS

The Aerospace Corporation functions as an "architect-engineer" for national security programs, specializing in advanced military space systems. The Corporation's Technology Operations supports the effective and timely development and operation of national security systems through scientific research and the application of advanced technology. Vital to the success of the Corporation is the technical staff's wide-ranging expertise and its ability to stay abreast of new technological developments and program support issues associated with rapidly evolving space systems. Contributing capabilities are provided by these individual Technology Centers:

Electronics Technology Center: Microelectronics, solid-state device physics, VLSI reliability, compound semiconductors, radiation hardening, data storage technologies, infrared detector devices and testing; electro-optics, quantum electronics, solid-state lasers, optical propagation and communications; cw and pulsed chemical laser development, optical resonators, beam control, atmospheric propagation, and laser effects and countermeasures; atomic frequency standards, applied laser spectroscopy, laser chemistry, laser optoelectronics, phase conjugation and coherent imaging, solar cell physics, battery electrochemistry, battery testing and evaluation.

Mechanics and Materials Technology Center: Evaluation and characterization of new materials: metals, alloys, ceramics, polymers and their composites, and new forms of carbon; development and analysis of thin films and deposition techniques; nondestructive evaluation, component failure analysis and reliability; fracture mechanics and stress corrosion; development and evaluation of hardened components; analysis and evaluation of materials at cryogenic and elevated temperatures; launch vehicle and reentry fluid mechanics, heat transfer and flight dynamics; chemical and electric propulsion; spacecraft structural mechanics, spacecraft survivability and vulnerability assessment; contamination, thermal and structural control; high temperature thermomechanics, gas kinetics and radiation; lubrication and surface phenomena.

Space and Environment Technology Center: Magnetospheric, auroral and cosmic ray physics, wave-particle interactions, magnetospheric plasma waves; atmospheric and ionospheric physics, density and composition of the upper atmosphere, remote sensing using atmospheric radiation; solar physics, infrared astronomy, infrared signature analysis; effects of solar activity, magnetic storms and nuclear explosions on the earth's atmosphere, ionosphere and magnetosphere; effects of electromagnetic and particulate radiations on space systems; space instrumentation; propellant chemistry, chemical dynamics, environmental chemistry, trace detection; atmospheric chemical reactions, atmospheric optics, light scattering, state-specific chemical reactions and radiative signatures of missile plumes, and sensor out-of-field-of-view rejection.